Journal of Catalysis 263 (2009) 4–15

Contents lists available at ScienceDirect

Journal of Catalysis

www.elsevier.com/locate/jcat

A novel method for preparing an active nickel phosphide catalyst for HDS of dibenzothiophene

J.A. Cecilia, A. Infantes-Molina, E. Rodríguez-Castellón, A. Jiménez-López *

Departamento de Química Inorgánica, Cristalografía y Mineralogía (Unidad Asociada al ICP-CSIC), Facultad de Ciencias, Universidad de Málaga, Campus de Teatinos, 29071 Málaga, Spain

ARTICLE INFO

Article history:
Received 17 November 2008
Accepted 10 February 2009
Available online 26 February 2009

Keywords:
Mesoporous MCM-41
Nickel phosphide (Ni_2P)
Dibenzothiophene
HDS

ABSTRACT

Ni_2P catalysts supported on mesoporous silica (MCM-41) were prepared by temperature programmed reduction through a novel method using nickel(II) dihydrogenphosphite, $Ni(HPO_3H)_2$, as a precursor salt, and preparing three catalysts with nickel loadings of 5, 10 and 15 wt% denoted as Ni_2P-*x*, where *x* is the percentage in weight of nickel. X-ray diffraction (XRD), X-ray photoelectron spectroscopy (XPS) and N_2 adsorption–desorption isotherms were used to study the formation of the phase. The dibenzothiophene (DBT) hydrodesulfurization (HDS) activity was measured for Ni_2P-*x* catalysts and they showed good TOF values at 400 °C. The conversion hardly changes with the metallic loading, and increases with temperature in all cases. On the other hand, Ni_2P-5 catalyst shows a better intrinsic activity of Ni_2P phase. Further, an improvement in the activity is found with time on stream, where an increase in both stability and activity are observed, reaching conversions of close to 95%. XRD and XPS analysis of spent catalysts show that the formation of a more active Ni_2P phase takes place under the reaction conditions. The support impregnated with nickel(II) dihydrogenphosphite, without prior reduction, was also active in this reaction, increasing in activity with time on stream as a consequence of the formation of the corresponding Ni_2P or other mixed NiP_xS_y phases under the experimental conditions.

1. Introduction

Sulfur removal from petroleum feedstocks is becoming one of the most significant issues in the refinery industry because of recently enacted environmental protection laws. Reducing the level of sulfur in diesel fuel will increase the durability and performance of after-treatment technologies used in automobiles to satisfy the stringent clean air standards established globally. Sulfur in fuels is a pollutant, and reduction of sulfur beyond current requirements is beneficial from both an air quality and pollution control equipment standpoint. Existing EPA rules (*AEO2008*) requires that 80 percent of highway diesel supplies contain no more than 15 ppm sulfur for the period 2006–2010. After 2011 all highway diesel is required to contain less than 15 ppm sulfur [1]. The need to find a solution for this considerable problem has led to a worldwide search for appropriate hydrodesulfurization catalysts.

Traditionally, hydrotreating catalysts are based on molybdenum or tungsten sulfide and promoted by cobalt or nickel as the active phases with mainly porous γ-alumina as a material support. Many efforts have been devoted to achieving an optimum performance of these sulfide systems, although the nature of the active phase has hardly been modified [2,3], i.e. Mo(W)S_2 slabs edge-decorated with cobalt or nickel.

The use of phosphorous as hydroprocessing catalyst promoter has been extensively researched, and the effect of phosphorous in sulfide catalysts widely studied by many workers [4,5]. Phosphorous, as phosphate, mainly alters the acid–base properties of the material support, which is directly correlated to the active phase dispersion [6]. Prins suggested a possible formation of a nickel and/or molybdenum phosphide at the edges of the MoS_2 [7], and Magnus et al. reported the modification by phosphorous of the reaction mechanism [8]. Other authors have pointed out that the cobalt (or nickel) sulfide may act as the catalyst itself, instead of acting as the promoter of the molybdenum (or tungsten) sulfide based catalysts [9].

Based on these premises, together with the knowledge that the catalytic properties of transition metals can be greatly modified by combining them with main group elements, workers in the field have opened up new frontiers of research by developing catalytic systems which combine transition metals such as Ni, Co, Mo, W with N (nitrides) [10,11], C (carbides) [12,13] and recently P (phosphides), such as MoP [14], WP [14,15] and Ni_2P [16–22], as the active phases in HDS and HDN reactions.

Catalysts with Ni_2P as an active phase have been shown not only to have better catalytic results than Ni sulfide, which has a low HDS activity [23–26], but also to be better than the traditional

* Corresponding author. Fax: +34 952137534.
E-mail address: ajimenezl@uma.es (A. Jiménez-López).

0021-9517/$ – see front matter
doi:10.1016/j.jcat.2009.02.013

sulfide catalysts [21]. Further, it has been reported that the activity in 1-butene hydrogenation follows the order $Ni_2P > Co_2P > FeP$ [27]. In HDS and HDN reactions, the activity was in the order $Ni_2P > WP > MoP > CoP > Fe_2P$ [19]. These phosphide based catalysts are becoming an interesting and promising replacement for the traditional bimetallic systems such as Mo or W sulfide catalysts promoted with Ni or Co in this type of reaction. This approach provides considerable economical advantages as well as enhanced catalyst life times and higher activity.

These phosphides have been classified based on the stoichiometry, i.e., metal rich phosphides (M/P > 1), monophosphides (M/P = 1), and phosphorous rich phosphides (M/P < 1). Monophosphides and metal rich phosphides display better properties, i.e., hardness, high thermal and electrical conductivity and thermal stability [28].

There have been different approaches to preparing nickel phosphide catalysts such as solid state reactions of metal and phosphorous [29], or the electrolysis of fused salts [30], although the need for extreme conditions, such as high temperatures and pressures, have limited their application. Many investigations have dealt with the preparation of such phosphides by temperature programmed reduction, where a great variety of experimental parameters were imposed i.e., changes in the Ni/P ratio, the heating rate, the hydrogen flow and the temperature conditions. These variations resulted in the formation of nickel phosphides with different stoichiometries ($Ni_{12}P_5$, Ni_5P_4, which were less active than the Ni_2P itself) [17,31,32]. Nickel phosphide supported catalysts have been prepared mainly by impregnation of the support with $(NH_4)_2HPO_4/NH_4H_2PO_4$ and $Ni(NO_3)_2$ solutions, then dried and calcined to obtain the nickel phosphate precursor [17,21]. After a subsequent temperature programmed reduction the desired nickel phosphide is formed. The Ni/P atomic ratio added has a profound impact on the structure and activity of nickel phosphide based catalysts, mainly effecting the HDN reactions. With regard to this, Prins et al. [14] have reported that a Ni/P ratio between 2 and 1.3 is necessary to synthesize Ni_2P/SiO_2, while lower amounts of phosphorous lead to the formation of $Ni_{12}P_5$ and Ni_3P phases. The temperature programmed reduction method demands high temperatures in order to reduce the phosphate species, mainly due to the strong P–O bond in the phosphate. Korányi [22] as well as Berhault and coworkers [33] have prepared nickel thiophosphate ($NiPS_3$) to generate unsupported nickel phosphides at lower temperatures. Yang et al. [34] prepared phosphide based catalysts by treating reduced metal particles with phosphine, obtaining highly dispersed metal-phosphide particles. Schaak [35] and Chiang [36] have reported that metallic Ni nanoparticles could be transformed into Ni_2P by treatment with TOP (trioctylphosphine).

In this paper we describe the preparation of Ni_2P catalysts through an easier and novel process which improves the current preparation method employing phosphate-containing precursors and high reduction temperatures (570–650 °C). For this, phosphorous acid and nickel(II) hydroxide were chosen as phosphorous and nickel precursors, respectively. These are reacted to form the $Ni(HPO_3H)_2$ salt, so that the starting material for forming the desired Ni_2P is a salt which possesses a lower phosphorus oxidation state than that reported in the literature to form the same compound. As a consequence it should be easier to reduce and to form the desired phosphide. MCM-41 was chosen as support [37] since, due to its textural properties, it is easy to obtain a highly dispersed Ni_2P phase. This synthetic route provides several very important advantages with regards to the published methods in the literature for forming an active Ni_2P phase; the addition of phosphorous and nickel takes place in only one step, there is no need for calcination and a lower reduction temperature and lower H_2 flows are permissible for forming the phosphide phase.

2. Experimental

2.1. Preparation of catalysts

The catalyst support used to prepare nickel phosphide based catalysts was the traditional mesoporous silica (MCM-41). Phosphorus and nickel were introduced by the incipient wetness impregnation method but using a new precursor for nickel and phosphorous different to those traditionally used to obtain this type of phosphide. A solution of nickel(II) dihydrogenphosphite ($Ni(HPO_3H)_2$) was prepared by adding the stoichiometric amounts of nickel(II) hydroxide and phosphorous acid (H_2PO_3H) to the incipient volume. Once the aqueous salt solution was added to the pelletized support (0.85–1.00 mm), it was air dried at 40 °C. Finally, a temperature programmed reduction was used to convert the phosphite into phosphide. For this purpose, the sample was placed in a tubular reactor, and different parameters such as heating velocity (1–3 °C min^{-1}), final temperature (375–425 °C) and hydrogen flow (100–200 ml min^{-1}) were studied in order to optimize the Ni_2P formation.

The concentration of the precursor solutions were adjusted to the desired metal loading. Three catalysts were prepared with a nickel loading ranging from 5 to 15 wt% of Ni. The prepared catalysts will be referred to as Ni_2P-*x*, where *x* represents the percentage in weight of nickel present in the sample.

2.2. Characterization of catalysts

Powder patterns were collected on a X'Pert Pro MPD automated diffractometer equipped with a Ge(111) primary monochromator (strictly monochromatic CuK_1 radiation) and an X'Celerator detector. Textural parameters were evaluated from the nitrogen adsorption–desorption isotherms at −196 °C as determined by an automatic ASAP 2020 system from Micromeritics. Elemental Chemical Analysis of carbon, hydrogen, nitrogen and sulfur (CNHS) was performed with a LECO CHNS 932 analyzer.

X-ray photoelectron spectra were collected using a Physical Electronics PHI 5700 spectrometer with non-monochromatic AlK_α radiation (300 W, 15 kV, and 1486.6 eV) with a multi-channel detector. Spectra of pelletized samples were recorded in the constant pass energy mode at 29.35 eV, using a 720 μm diameter analysis area. Charge referencing was measured against adventitious carbon (C 1*s* at 284.8 eV). A PHI ACCESS ESCA-V6.0 F software package was used for acquisition and data analysis. A Shirley-type background was subtracted from the signals. Recorded spectra were always fitted using Gaussian–Lorentzian curves in order to determine the binding energy of the different element core levels more accurately. Reduced and spent catalysts have been stored in sealed vials with an inert solvent. The sample preparation was done in a dry box under a N_2 flow, where the solvent was evaporated prior to the introduction into the analysis chamber and directly analyzed without previous treatment.

2.3. Catalytic test

For the catalytic test, the hydrodesulfurization of DBT was chosen, which was performed in a high-pressure fixed-bed continuous-flow stainless steel catalytic reactor (9.1 mm in diameter, and 230 mm in length), operated in the down-flow mode. The reaction temperature was measured with an interior placed thermocouple in direct contact with the catalyst bed. The organic feed consisted of a solution of DBT (3000 ppm) in decalin that was supplied by means of a Gilson 307SC piston pump (model 10SC). For the activity tests, 0.5 g of catalyst was used (particle size 0.85–1.00 mm) and was diluted with quartz sand to 3 cm^3. Prior to the activity test, the catalysts were reduced in situ at atmospheric pressure

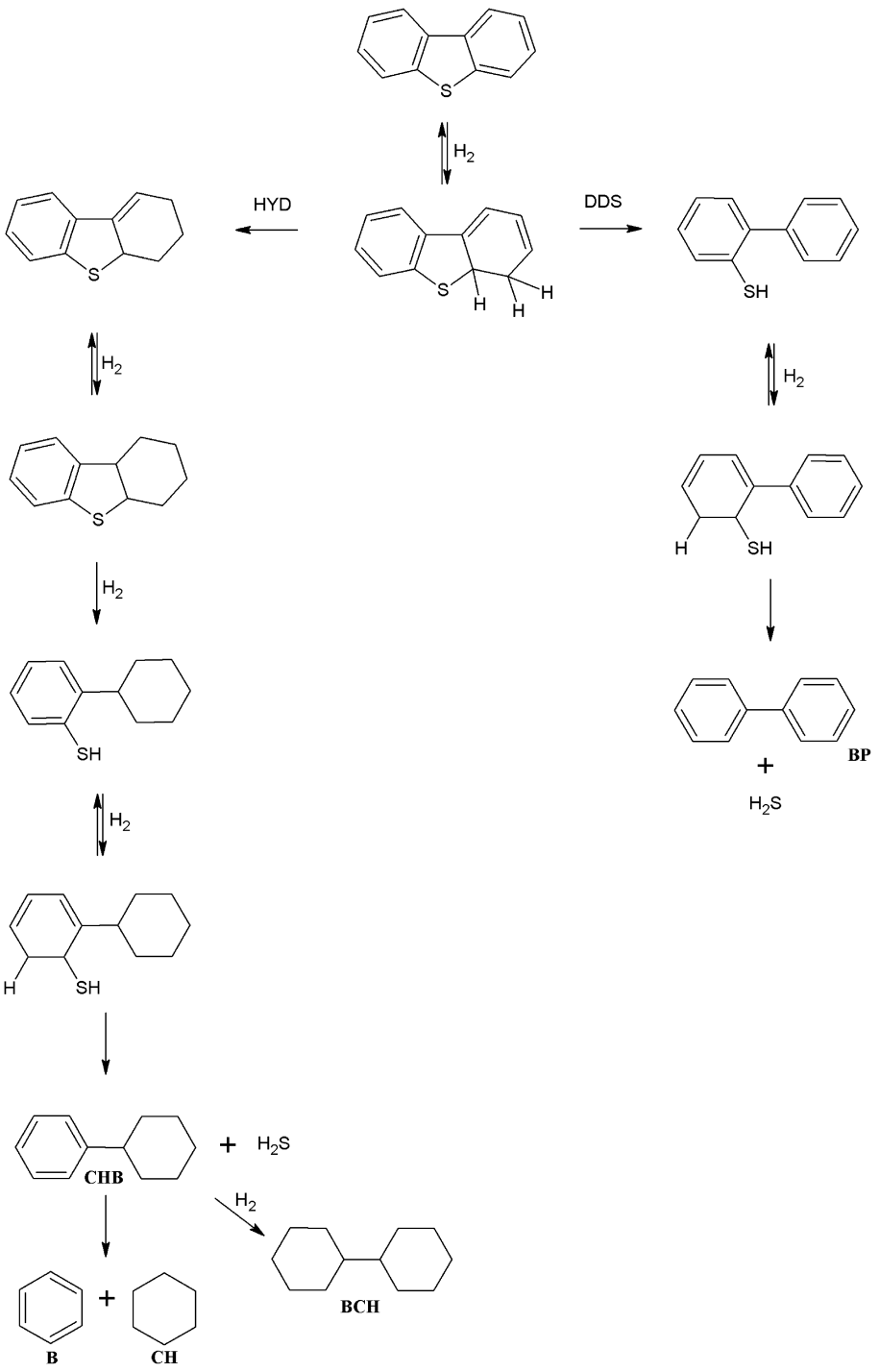

Scheme 1.

with a H_2 flow of 100 ml min^{-1} by heating from rt. to 375 °C at a heating rate of 3 °C min^{-1}. Catalytic activities were measured at different temperatures (300–400 °C), under 3.0 MPa of H_2, with a flow rate of 100 ml min^{-1} and with weight hourly space velocities (WHSV) of 32 h^{-1}. The evolution of the reaction was studied by collecting liquid samples after 60 min at the desired reaction temperature. The liquid samples were kept in sealed vials at room temperature and subsequently analyzed by gas chromatography (Shimadzu GC-14B, equipped with a flame ionization detector and a capillary column, TBR-14, coupled to an automatic Shimadzu AOC-20i injector). For these catalysts, the main products of the reaction were biphenyl (BP), cyclohexylbenzene (CHB), benzene (B) and cyclohexane (CH) as reflected in Scheme 1. For this reason, the total conversion was calculated from the ratio of converted dibenzothiophene/initial dibenzothiophene. The selectivity of different reaction products was calculated considering BP, CHB, B and CH as the only products obtained, since only traces of unknown compounds were noticeable in some cases.

Turn over frequencies values were calculated from the formula,

$$\mathrm{TOF} = \frac{F}{W}\frac{X}{M},$$

where F is the molar rate of reactant, W is the weight of catalyst, X is the conversion and M is the mole of sites loaded.

3. Results and discussion

3.1. XRD

As previously stated, several experimental parameters have been studied in order to optimize the procedure for the formation of a Ni_2P phase from the TPR reduction of a $Ni(HPO_3H)_2$ precursor. Heating rate and hydrogen flow have been considered in the same way as other authors for the preparation of Ni_2P from $NiHPO_4$.

A precursory trial was the synthesis of bulk Ni_2P by this new method. Stoichiometric quantities of nickel(II) hydroxide and phosphorous acid were dissolved in distilled water so as to form a light green solution of $Ni(HPO_3H)_2$. Water was evaporated by heating at 40 °C under moderate stirring to obtain a green solid. XRD of this sample did not show any diffraction line as long as $Ni(HPO_3H)_2$ compound is totally amorphous (Fig. 1A). Subsequently, the compound was heated from room temperature (rt.) to 100 °C at 10 °C min^{-1} under a flow of helium of 60 ml min^{-1} and maintained at this temperature for 45 min. Afterwards, it was heated to 800 °C at 3 °C min^{-1} under a H_2 flow of 150 ml min^{-1}. The XRD pattern of this unsupported sample (Fig. 1B) was similar to a reference pattern from the JCPDS powder diffraction file (Card No. 01-089-4864) as well as the XRD patterns reported by other authors [38] corresponding to the presence of Ni_2P. Therefore, this method lets prepare nickel phosphide phase in an easier way, i.e. nickel and phosphorous are added in one step and there is no need of calcination.

Once unsupported Ni_2P was obtained, the following step was to prepare the supported phase. A $Ni(HPO_3H)_2$ solution containing a 15 wt% of nickel was first prepared by combining stoichiometric amounts of nickel(II) hydroxide and phosphorous acid and then incorporating the solution on a MCM-41 support by the incipient wetness impregnation method. To start, as was done for unsupported nickel phosphide sample, XRD measurement of the precursor material was carried out i.e. the support impregnated with $Ni(HPO_3H)_2$. The corresponding diffractogram (not shown) does not show any diffraction peaks, as expected for this amorphous compound.

Several trials were carried out in order to optimize the experimental conditions to be used, so as to form the desired Ni_2P phase. First, the influence of the final reduction temperature was studied. After each treatment, a XRD measurement was made to observe the phases formed and their evolution. Fig. 2A shows the corresponding results. The pattern all show a broad feature at $2\theta = 25°$ due to the amorphous nature of mesoporous MCM-41 [37]. At temperatures below 350 °C no peaks were noticeable (not shown). At higher temperatures small signals corresponding to Ni_2P began to appear, increasing in their intensity with temperature. Because $Ni(HPO_3H)_2$ solid is amorphous, we cannot ruled out its presence at 350 °C, it is very possible that only a partial reduction of this compound took place. In fact, at higher temperatures (400 °C) the peaks of Ni_2P phase become more intense, even with new ones appearing, which could support the argument for the presence of unreduced $Ni(HPO_3H)_2$. An increase in the temperature leads to the formation of new phases as for TPR reduction of nickel phosphate. Thus at 400 and 425 °C, although the peaks corresponding to Ni_2P phase are more intense and well defined, new signals now become noticeable. The assignment of these new signals reveals the formation of $Ni(PO_3)_2$ (PDF Card No. 00-028-0708) and Ni_5P_4 (PDF Card No. 01-089-2588), the latter being a phosphorous rich phase and possibly favored at higher temperatures due to the excess of this element in the pristine compound, $Ni(HPO_3H)_2$. The reduction processes of Ni/P systems are not precisely described in the literature since they depend on a variety of experimental factors. Prins et al. [38] have pointed out the possible formation of volatile species such as elemental P (P_4) or phosphines (P_xH_y).

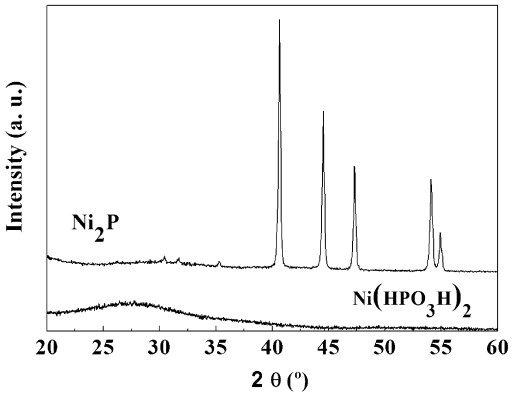

Fig. 1. X-ray diffractograms of (A) unsupported $Ni(HPO_3H)_2$ and (B) Bulk Ni_2P.

Phosphines are decomposed at higher temperatures to form P and H_2 that is catalyzed by nickel particles that are first reduced. This P reacts with nickel to form Ni_2P phase. Perhaps at higher temperatures greater proportions of phosphine is formed and react with nickel particles to form phosphorous rich phosphides such as Ni_5P_4, where the Ni/P ratio diminishes to 1.25. Therefore, the advantage of using $Ni(HPO_3H)_2$ as an initial compound to form Ni_2P is the low reduction temperature needed (375 °C) compared to a high temperature of 525 °C required when the starting substance is $NiHPO_4$ that, along with the no necessity of calcination, supposes an energy saving during the preparation process. Although it presents the disadvantage of forming mixed phases.

Reduction flow rate was also studied, changing the flow from 100 to 200 ml min^{-1}, and the corresponding results are shown in Fig. 2B. Few differences were found. Only by using the highest flow, were the peaks due to $Ni(PO_3)_2$ are noticeable. From these results, it can be seen that the undesired phase formations are favored at higher temperatures and higher flow rates, while the diffraction lines of nickel forming the Ni_2P phase are hardly modified. This is in contrast to the preparation of this phase by TPR of phosphate precursors. For this reason, the lowest flow rate was chosen for the preparation of Ni_2P using this new method. It has been reported that high flow rates favor the quick removal of water formed during the reduction process [39] leading to the formation of smaller particles as well as favoring diffusion of volatile P species onto nickel particles to form the phosphide. Stinner et al. [16] consider that an increase in the flow rate provokes a decrease in local partial pressure of volatile phosphorous species and water removal, the latter being essential in the preparation of these phosphides. However, we have not found any noticeable differences.

A variation in the heating rate was also carried out (Fig. 2C). As previously stated, a high gas space velocity and a low heating rate during temperature programmed reduction are necessary to prepare high-performance transition-metal carbides, nitrides and phosphides, and the removal of local water vapor from catalyst surface being a key factor to be considered. From this figure, few differences can be observed. Firstly, the intensity and sharpness of the peaks corresponding to Ni_2P phase increase as the heating rate is lowered. This is what would be expected if we consider that the crystallinity is favored when the time of formation of such a phase is longer, i.e., with 1 °C min^{-1}, and therefore favoring a more ordered structural organization. At 1 and 5 °C min^{-1} not only is the Ni_2P phase noticeable, but $Ni(PO_3)_2$ and Ni_5P_4 also appear. At 1 °C min^{-1}, along with the peaks corresponding to Ni_2P, $Ni(PO_3)_2$ is the another phase detected, the peaks of Ni_2P compound being the sharpest and most intense. Hence at a low heating rate a higher degree of crystallization takes place. On the other hand, at 5 °C min^{-1}, small diffraction lines due to Ni_5P_4 can also be ob-

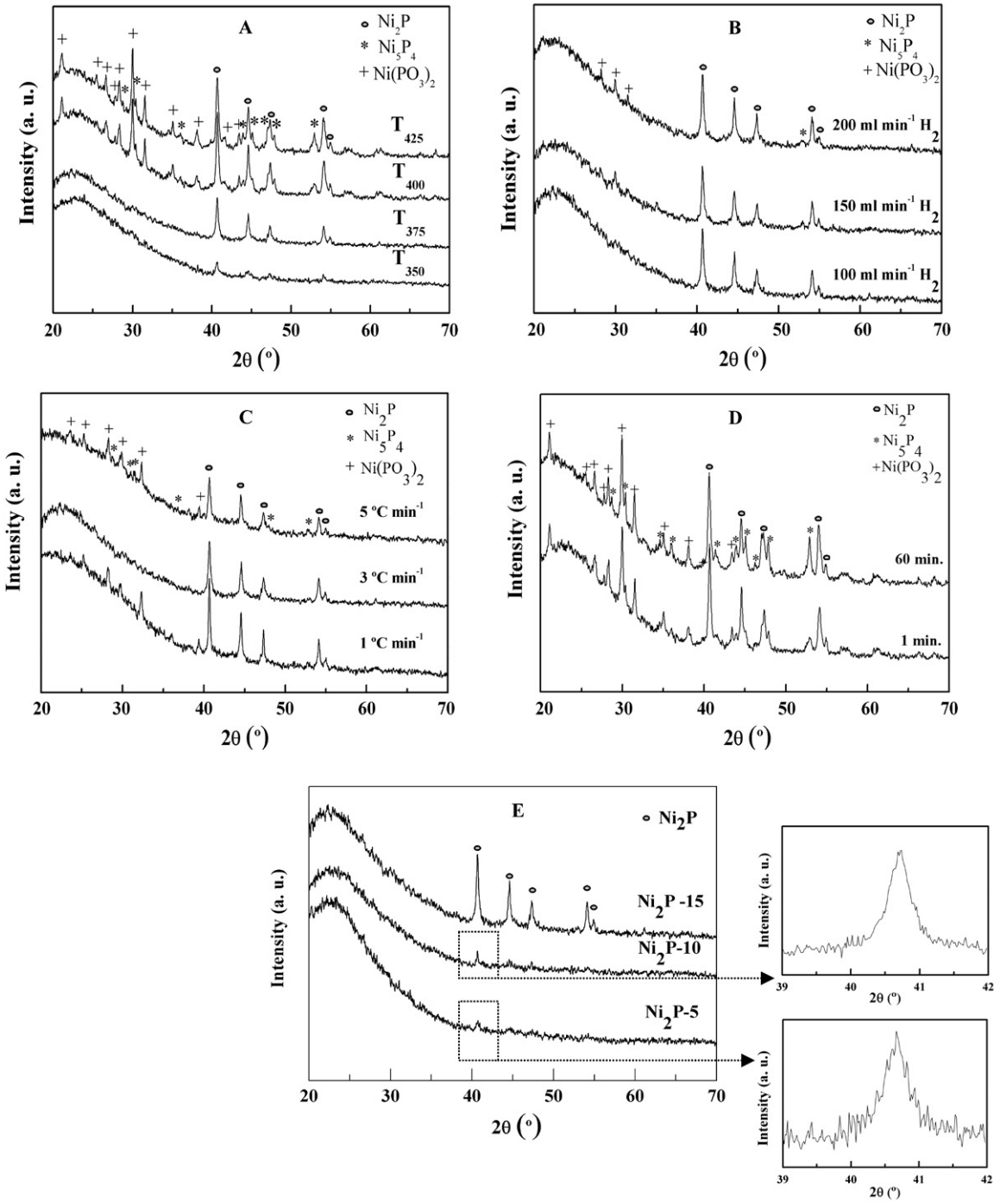

Fig. 2. X-ray diffractograms of: (A) Ni_2P-15 catalyst, reduced at different temperatures. H_2 flow: 100 ml min^{-1}, heating rate: 3 °C min^{-1}; (B) Ni_2P-15 catalyst, reduced under different flows. T^a: 375 °C, heating rate: 3 °C min^{-1}; (C) Ni_2P-15 catalyst, reduced under different heating rates. H_2 flow: 100 ml min^{-1}, T^a: 375 °C; (D) Ni_2P-15 catalyst with different reduction times at the desired temperature. H_2 flow: 100 ml min^{-1}, T^a: 400 °C, heating rate: 3 °C min^{-1}; (E) Ni_2P-*x* catalysts. H_2 flow: 100 ml min^{-1}, T^a: 375 °C, heating rate: 3 °C min^{-1}.

served. At 3 °C min^{-1} the Ni_2P phase is the only noticeable one, this heating rate being the optimum one to achieve our aim.

Another parameter studied was the time the sample was kept at the final reduction temperature. 400 °C was chosen in order to observe the evolution of the peaks corresponding to Ni_5P_4 and $Ni(PO_3)_2$ since at 375 °C they do not appear. Fig. 2D shows the results, indicating that an increase in intensity of the diffraction lines of the Ni_5P_4 phase occurs while those of the $Ni(PO_3)_2$ phase are hardly modified. Ni_2P diffraction lines increase slightly. The use of pure H_2 can provoke a local heating synterizing of some particles [16], especially if maintained at a high temperature for a long period of time. From Fig. 2D it can be deduced that with only one minute at the desired temperature both syntherization and formation of undesired phases can be avoided.

Finally, the metal loading was varied, with values ranging from 5 to 15 wt% of nickel. The reduction process conditions were set at a H_2 flow of 100 ml min^{-1}, a heating rate of 3 °C min^{-1} and a reduction temperature of 375 °C. The corresponding results are shown in Fig. 2E. Only the sample with the highest metal loading exhibits well defined Ni_2P diffraction lines in the X-ray diffrac-

togram, indicating that an extensive formation of such a phase takes place. The diffractograms of Ni_2P-5 and Ni_2P-10 samples only have a few diffraction lines corresponding to the most intense reflection of Ni_2P compound located at $2\theta = 40.7°$. It cannot be ruled out that in the Ni_2P-15 sample the formation of the desired phosphide starts to occur earlier, as its higher metallic loading provokes a weaker interaction with the material support. The former Ni_2P particles could act as nucleation sites where hydrogen is activated and therefore the reduction process is favored. The metallic character of Ni_2P should be kept in mind, as reported by some authors [16], due to the short Ni–Ni metal distance in Ni_2P phase (2.60 Å [40]), close to that of the pure metal (2.49 Å [41]). Crystallite sizes were calculated by using the Scherrer equation with the main diffraction line located at $2\theta = 40.7°$. In order to perform such a measurement, XRD for Ni_2P-5 and Ni_2P-10 catalysts were re-run between $2\theta = 38°$ and 42° increasing the counts number and with a high resolution optic. Crystal sizes of 50, 58 and 56 nm were obtained for Ni_2P-5, Ni_2P-10 and Ni_2P-15, respectively. The increasing metal loading does not alter the particle size.

3.2. Textural properties

Table 1 summarizes the textural properties of Ni_2P-*x* supported catalysts. It should first be noted that these catalysts suffer a considerable loss of surface area and pore volume. Some authors have pointed to a shrinkage in the structure as a consequence of the formation of a phosphosilicate [14] and that the phosphide particles are embedded in the silica support after the reduction conditions, making the mesopores inaccessible to gas molecules. In fact, the XRD peak at lows angles is hardly detectable, what seems to indicate a partial destruction of the MCM-41 support. Notwithstanding, from N_2 adsorption–desorption isotherms (not shown) the mesoporous feature is maintained for Ni_2P-5 and Ni_2P-10 catalysts, meanwhile Ni_2P-15 catalyst losses it. Ni_2P-15 possesses a precursor loading (Ni + P) of 30 wt%, what provokes a destruction of the mesoporous structure. In the same way, Abu et al. [42] have found the same behavior; metal phosphides supported on MCM-41 have much lower surface areas than pristine MCM-41, indicating that some of the MCM structure is lost during the preparation of metal phosphide. The low surface area of these materials could be due to the formation of Ni_2P particles on the external surface which impedes the access of N_2 molecules to mesoporous structure. Sun et al. [43] reported that a Ni_2P/SiO_2 catalyst gave the highest activity but the lowest S_{BET} value, revealing the absence of a correlation between the surface area and the HDS activity with this type of active phase. In this context, it is the Ni_2P-10 catalyst, with a surface area of 38.4 $m^2\,g^{-1}$, which displays the highest catalytic activity at moderate temperatures, corroborating this finding.

Table 1
Textural properties of the support and catalysts.

Sample	S_{BET} ($m^2\,g^{-1}$)	V_p ($cm^3\,g^{-1}$)	d_p (av) (nm)
MCM-41	525	0.32	2.4
Ni_2P-5	87.3	0.06	2.9
Ni_2P-10	38.4	0.04	3.8
Ni_2P-15	22.7	0.04	6.3

3.3. XPS

In order to gain further insight into the surface composition of catalyst precursors, catalysts and spent catalysts, XPS technique was employed. Table 2 shows the binding energy values and Ni/P and Ni/Si atomic ratios for all the samples.

As a starting point, XPS spectrum for bulk Ni_2P (prepared by this new method) was carried out. Fig. 3 shows the Ni 2*p* and P 2*p* core level spectra. Ni 2*p* core level spectrum involves two contributions (Fig. 3A). The first one, is assigned to $Ni^{\delta+}$ in Ni_2P phase and centered at 852.6 eV [44], and a second one is at 856.4 eV, corresponding to Ni^{2+} ions interacting possibly with phosphate ions as a consequence of a superficial passivation, along with the broad shake-up peak at approximately 6.0 eV above the Ni^{2+} species [45]. This satellite is due to divalent species [45,46], although in the literature has also been assigned to trivalent and oxysulfided nickel species [47]. Meanwhile, with regards to P $2p_{3/2}$ binding energy, it has been reported to be 129.5 eV for $P^{\delta-}$ on metal phosphides [48] and 133.5 for surface metal phosphate species [49], due to the superficial oxidation of nickel phosphide bulk particles. The spectra corresponding to the bulk sample (Fig. 3B) confirms this finding, with the corresponding bands at 129.3 and 133.5 eV for both kinds of phosphorous derivatives.

In order to investigate the Ni 2*p* core level spectra of MCM-41 supported catalysts, the analysis of Ni 2*p* signal of Ni_2P-15 sample was considered as representative. Fig. 4A plots the corresponding spectra of precursor and reduced sample, respectively. The precursor spectrum shows two Ni $2p_{3/2}$ signals, one with a binding energy value of 856.8 eV, as shown in Table 2, and another one of the broad shake-up satellite. We have assigned the main peak to Ni^{2+} ions mainly forming $Ni(HPO_3H)_2$ since XRD results show the absence of any other nickel species and the preparation procedure of such a precursor is not expected to modify nickel and

Table 2
Spectral parameters obtained by XPS analysis.

Sample	Binding energy (eV)					Superficial atomic ratio	
	Ni $2p_{3/2}$		P $2p_{3/2}$				
	Ni^{2+}	Ni_2P	HPO_3H^-	PO_4^{3-}	Ni_2P	Ni/P	Ni/Si
Ni_2P Bulk	*856.1*	*852.6*	*133.5*	–	*129.3*		
			Precursors				
Ni_2P-5	856.8	–	133.3	–	–	0.35	0.10
Ni_2P-10	856.6	–	133.5	–	–	0.55	1.48
Ni_2P-15	856.4	–	133.3	–	–	0.51	1.55
			Catalysts				
Ni_2P-5	857.4	853.7	133.3	134.5	–	0.23	0.12
Ni_2P-10	857.2	853.1	133.6	134.7	–	0.11	0.08
Ni_2P-15	856.9	852.8	133.2	134.7	–	0.20	0.21
			Spent catalysts				
Ni_2P-5	–	–	133.4	–	129.1	0.04	0.01
Ni_2P-10	856.9	853.0	133.7	–	129.4	0.42	0.24
Ni_2P-15	856.6	852.9	133.6	–	129.1	0.45	0.66
Ni_2P-10 (48 h)	856.8	853.4	133.2	134.6	129.7	0.53	0.32
$Ni(HPO_3H)_2$/MCM-41	856.8	852.8	133.4	–	129.5	0.08	0.17

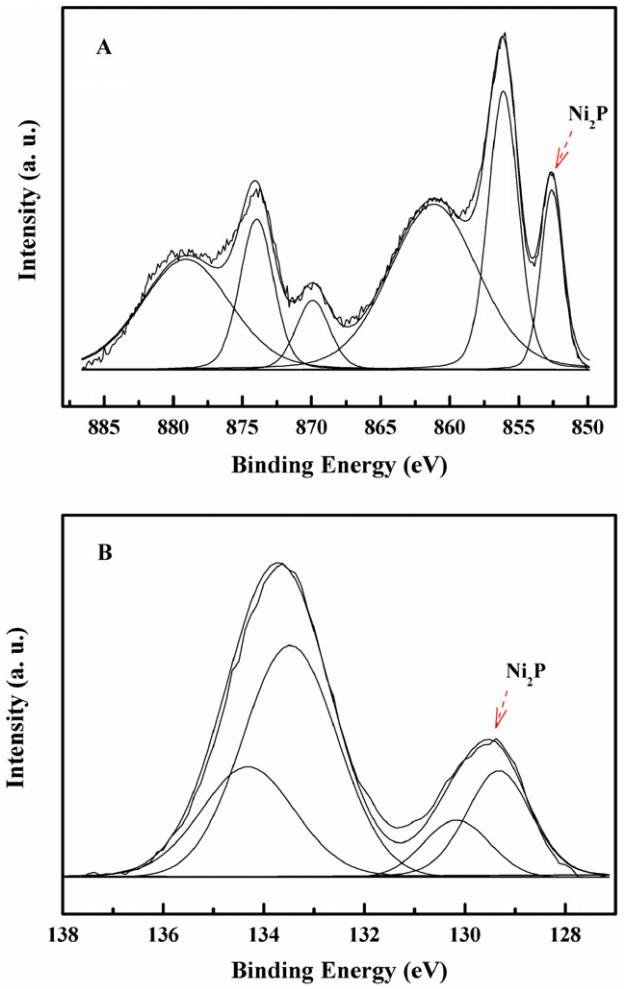

Fig. 3. XPS spectra for Ni_2P-10 bulk sample: (A) Ni 2*p* core level spectra and (B) P 2*p* core level spectra.

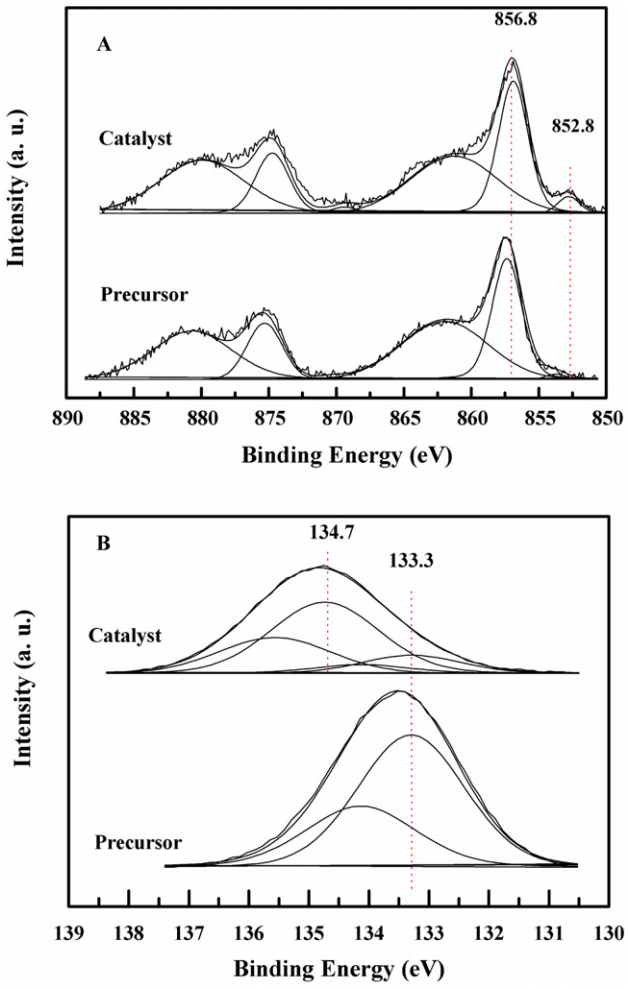

Fig. 4. XPS spectra for Ni_2P-15 precursor and catalyst: (A) Ni 2*p* core level spectra and (B) P 2*p* core level spectra.

phosphorus species. The Ni 2*p* signal for catalysts also possess a small band located at 852.8 eV, assigned to $Ni^{\delta+}$ forming Ni_2P, as seen from the bulk sample spectrum. If we compare this band for catalysts with varying nickel content, its intensity increases with nickel and phosphorous content (not shown), while the binding energy value follows the opposite trend as can be seen in Table 2, where Ni_2P-5 sample has a value of 853.7 eV, which is nearly 1 eV higher than that of Ni_2P-15, 852.8 eV. The oxidation states of Ni and P in Ni_2P are not clearly established, although it has been reported that Ni has a positive charge and P a negative one. The Ni 2*p* forming Ni_2P has a binding energy value very close to that reported for Ni^0 species (852.0–853.0 eV) [45]. The binding energy of this band at higher metallic loading shifts to lower values, and could be due to a lower interaction of Ni_2P compound with the material support.

Similarly, the P $2p_{3/2}$ signal for Ni_2P-15 sample is shown in Fig. 4B for the catalyst precursor and the catalyst. If we consider the precursor spectra, the P $2p_{3/2}$ signal is centered at 133.3 eV, which is assigned to phosphorous in the form of HPO_3H^-, as previously reported [48], so long as no treatment has been carried out during the preparation procedure to modify the oxidation state of phosphorous. However, after the reduction process a small band at 129.5 eV is observed as was found in bulk Ni_2P, while the band at 133.2 eV remains, albeit with a lower intensity, which confirms the above supposition that phosphite ions are not totally reduced under the experimental conditions, while a new band at 134.7 eV is clearly observed, and assigned in the literature to phosphate species [22]. This conclusion could be refuted by the results obtained by XRD, where the diffraction lines of phosphate compounds were not observed. Besides, Ni 2*p* signal corresponding to nickel phosphide is clearly identified. This could indicate that phosphorous on such a phosphide is located below a superficial layer of phosphate produced by oxidation/passivation in air. The BE of the phosphate band on supported samples has a displacement of 1 eV to a higher BE with regards to unsupported sample. The greater interaction with the material support would be responsible for such a shift.

XPS analyses were also used to calculate the surface Ni/P and Ni/Si atomic ratios (Table 2). If we consider the superficial Ni/P ratio, the theoretical ratio corresponding to precursor materials would be 0.5, assuming that $Ni(HPO_3H)_2$ is the compound present on the surface. Ni_2P-15 and Ni_2P-10 have such a ratio, while Ni_2P-5 has a lower value. After reduction, this ratio diminishes considerably, when it should have increased if Ni_2P compound were being formed. Taking into account that the experimental conditions used to obtain Ni_2P are very gentle, it is not possible to expect a loss of phosphorous in the form of PH_3; the low Ni/P ratio found for the catalysts confirms that on the surface there is an enrichment of phosphorous, although it is essentially present as $(HPO_3H)^-$ remnants and PO_4^{3-} forming a passivation layer in the surface of Ni_2P particles. Ni_2P-10 sample gives the lowest Ni/P and Ni/Si ratios after the reduction process.

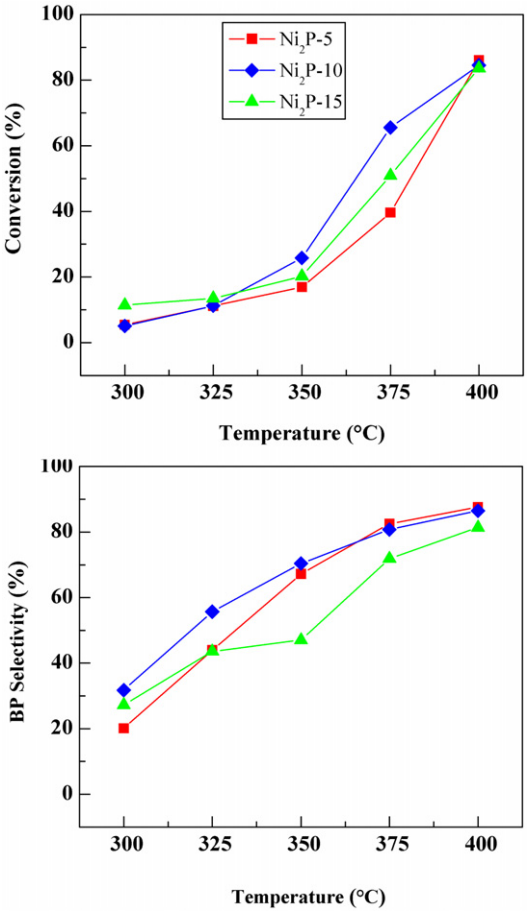

Fig. 5. Plots of conversion and BP selectivity versus T^a for Ni_2P-x catalysts.

Table 3
Activity data and Ni_2P properties of reduced and spent catalysts.

	Catalytic results						
	Ni_2P-5	Ni_2P-10	Ni_2P-15		Ni_2P-5	Ni_2P-10	Ni_2P-15
	Conversion (%)				Dc (nm)[a]		
Initial	5	5	11	Reduced[a]	50	58	56
At 400 °C	86	85	84	Spent[b]	51	86	86
	Selectivity (%) at 400 °C				Metal site concentration (μmol g^{-1})		
B	3	5	14	Reduced	18	21	32
BP	88	87	73	Spent	18	31	49
					TOF × 10^3 (s^{-1})		
CHB	7	7	11	Initial	0.44	0.35	0.34
BCH	2	1	2	At 400 °C[c]	7.1	5.8	3.9

[a] Calculated from the most intense reflection of Ni_2P of XRD results (Scherrer equation).
[b] At the beginning of the reaction.
[c] After reaction at 400 °C.

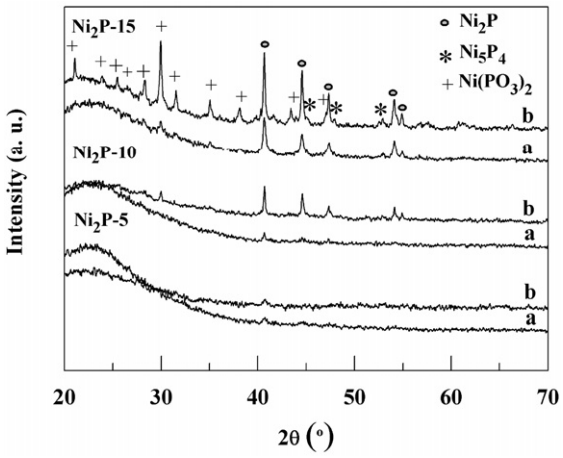

Fig. 6. X-ray diffractograms of (a) reduced and (b) spent Ni_2P-x catalysts after the temperature test.

3.4. Catalytic results

Firstly, the activity related to the amount of nickel and phosphorous present in the catalyst was studied, using MCM-41 as support. Results from DBT HDS are plotted in Fig. 5. The conversion of DBT yields mainly biphenyl by direct hydrogenolysis or direct desulfurization, DDD (Scheme 1). Products resulting from hydrogenation reaction (CHB) and cracking reactions (B) are also detected but in minor quantities. It has been also reported a lower hydrogenation activity of phosphides, with regards to sulfides, indicating a more effective use of hydrogen [19] in the HDS reaction. A study using the Ni–Mo–P/SiO_2 catalyst [43] underlined the importance of nickel sites in Ni_2P in the catalytic activity, concluding that HDS reaction mainly occurred on Ni sites, this being one of the properties that makes phosphide catalysts different from either sulfide, carbide or nitride catalysts.

In all cases, the conversion values are practically the same at low and high temperatures, however, at 350 and 375 °C, the Ni_2P-10 sample exhibits the highest conversion values. No information can be gained from XRD and S_{BET} data to explain such behavior. However, according to XPS atomic ratio (Table 2), if we consider Ni/P and Ni/Si ratios, we notice how this catalyst has the lowest initial value, which would suggest a different distribution of the active phase on the surface. Bussell et al. have indicated that P species in Ni_2P/SiO_2 catalysts increases the dispersion of nickel on silica support [50]. As exposed earlier, they all present similar particle sizes. It can be seen, from the results plotted in Fig. 5, that there are no great differences between these three catalysts. The fact that at higher temperatures all the catalysts reach the same conversion value led us to think about the possibility of a substantial change taking place over the surface during the catalytic test, causing all of their equivalent Ni_2P sites to reach the same level of activity. If this were the case, it could be said that only a partial amount of nickel and phosphorous is transformed into active phosphide during the reduction process, prior to the catalytic test. Table 3 compiles the catalytic results at 400 °C, where similar conversion and selectivities are obtained.

XRD of spent catalysts were carried out in order to gain further insight into the possible active phase modification. Fig. 6 shows X-ray diffractograms in order to compare reduced and spent catalysts after the temperature test. It can be observed how the Ni_2P diffraction lines increase for Ni_2P-10 and Ni_2P-15 catalysts after reaction. From these results we can assume the formation of more Ni_2P phase and we can assess its higher crystallinity by calculating the particle size. These data reveal (Table 3) that Ni_2P-10 and Ni_2P-15 spent catalysts reach a size of 86 nm (Table 3). Further, over the Ni_2P-15 sample, new diffraction lines of $Ni(PO_3)_2$ and Ni_5P_4 appear. It seems that an excess of metallic loading is present over this sample, where, in addition to Ni_2P phase, a large proportion of nickel and phosphorous are forming undesired phases. Likewise, Ni_2P-10 spent catalyst also shows the main diffraction line of $Ni(PO_3)_2$ compound, although to a much lower extent. Finally, the sample with the lowest metallic loading, Ni_2P-5, does not reveal any apparent modification of Ni_2P phase. In this sense, a very weak diffraction line of Ni_2P phase is observed for both reduced and spent catalyst, but not an increased intensity of the Ni_2P phase is observed, possibly due to the low nickel loading of this sample. The particle size does not change (50 nm). Therefore, Ni_2P-5 sample apparently possesses enough Ni_2P phase to achieve

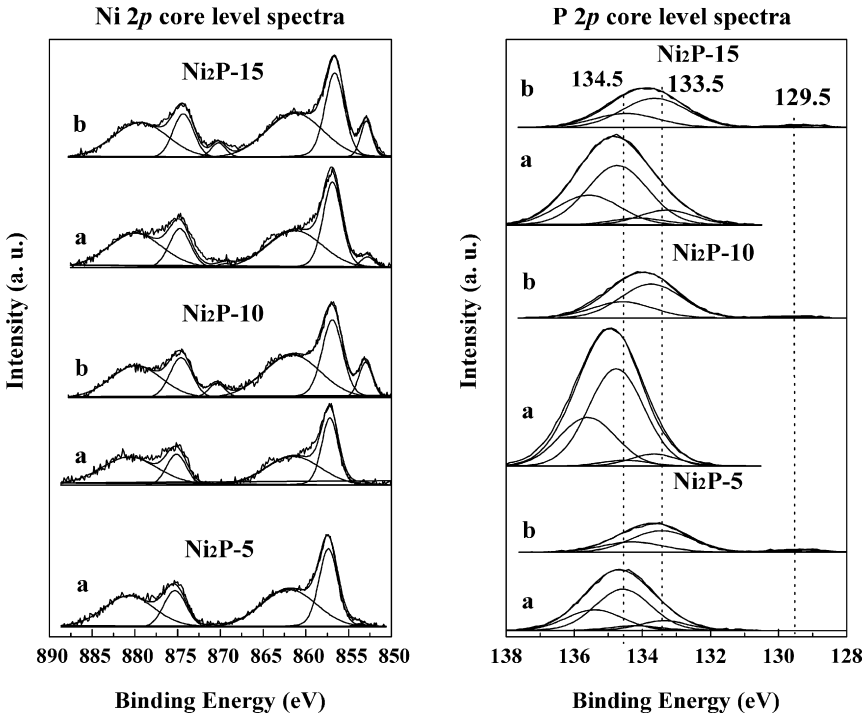

Fig. 7. Ni 2*p* and P 2*p* core level spectra for Ni_2P-10-*x* catalysts: (a) reduced catalysts and (b) spent catalyst after temperature test.

the same levels of activity than samples with higher nickel and phosphorous loadings.

The role of the metallic loading on catalytic activity is clarified if TOF values are calculated on the basis of the number of accessible sites. Toward this end, metal site concentration, assuming that the samples were composed of uniform spherical particles, was calculated and the corresponding data included in Table 3. Metal site concentration has been calculated as reported by Oyama et al. [51]. TOF values have been obtained at the beginning and the end of the reaction and they increase considerably. Ni_2P-5 possesses the highest activity what indicates a higher effectiveness of Ni_2P phase on this sample and therefore an excess of loading seems to be present on Ni_2P-10 and Ni_2P-15 catalysts, which remains unreduced or forming undesired phases such as Ni_5P_4 and/or $Ni(PO_3)_2$. From XRD results and TOF values it can be concluded that Ni_2P-5 sample possesses most of its metallic loading forming small Ni_2P particles which turn to be as active as bigger Ni_2P particles present on Ni_2P-10 and Ni_2P-15 catalysts. These results agree well with those reported by Oyama et al. [17] who pointed out the small effect of phosphorous content on conversion in HDS reactions, and suggested that the reaction mainly takes place on metal centers whose size hardly modifies the reactivity, i.e. the reaction is structure insensitive and occurs by direct sulfur removal from dibenzothiophene. Higher metallic loading favors the formation of higher crystallite sizes during the catalytic run.

Turn over rates obtained with this set of catalysts are good and their reliability can be compared with data published earlier. TOF for DBT HDS over Ni_2P/SiO_2 catalysts were 0.0015 s^{-1} [51] and 0.003 s^{-1} [43], respectively, lower than that presented here. The group of Korányi [52], in a study of Ni_2P supported on another mesoporous material such as SBA, the most active catalyst had an intrinsic hydrotreating activity of 0.0042 s^{-1} based in the same calculation. From these results we can conclude that the intrinsic activity of our catalysts is similar to or even higher than those reported in the literature.

To complete the study of spent catalysts, the analysis by XPS of Ni 2*p* and P 2*p* signals for spent catalysts are shown in Fig. 7. Ni 2*p* signal corroborates the results obtained with XRD measurements, where an increase in intensity of the peak at 852.8 eV corresponding to Ni_2P phase takes place for Ni_2P-10 and Ni_2P-15 spent catalysts, where an increase in the Ni/P ratio was also found. Similarly, the Ni/Si atomic ratio increases with regards to reduced samples, and there is a higher proportion of nickel over the surface after the test. However, it is surprising how the Ni 2*p* band for Ni_2P-5 spent catalyst was not detected from XPS. With regards to P 2*p* signal, a decrease in intensity is observed for all the spent catalysts, together with the disappearance of the band located at 134.5 eV. Only the band at 133.5 eV remains. Moreover, the band of Ni_2P species (129.5 eV) appears in all cases, confirming the XRD results for Ni_2P-10 and Ni_2P-15 samples. The formation of more Ni_2P phase under reaction conditions employed seems to be the clue of the increasing activity of these both samples in the temperature test. Notwithstanding, X-ray diffractogram for Ni_2P-5 catalyst did not show any change, which led us to conclude that more active Ni_2P phase is not formed over this catalyst. The appearance of the phosphide band in XPS spectra, along with the absence of the Ni 2*p* signal over the surface of this spent catalyst suggest the formation of another phase which is also active in this reaction. Ostensibly, the S 2*p* signal analysis for spent catalysts reflects that only Ni_2P-5 catalyst possesses two sulfur 2*p* bands located at 161.6 and 169.9 eV, which are due to sulfide and sulfate species respectively [53]. X. Duan et al. [54] have also observed two sulfur bands on a H_2S-passivated Ni_2P/MCM-41 catalyst which is active and stable in DBT HDS reaction. These authors have assigned the band at 169.9 eV as consequence of the oxidation of sulfur species retained on the Ni_2P/MCM-41 catalyst surface and in our case it should be a partial oxidation of the sulfur species responsible of the band at 161.6 eV. The amount of sulfur detected is very low, 0.84%, therefore only a partial surface sulfidation takes place, probably forming a NiP_xS_y phase on the surface of Ni_2P particles which is reported to be active in HDS reactions. The same authors [54] have underlined that a sulfur-associated surface reconstruction occurs in the course of HDS. This surface reconstruction should be the responsible of the quasi-imperceptible Ni 2*p* signal. If we considered XRD and XPS data for Ni_2P-5 catalyst, it possesses the lowest particle size along with the Ni 2*p* band corresponding to Ni_2P phase at

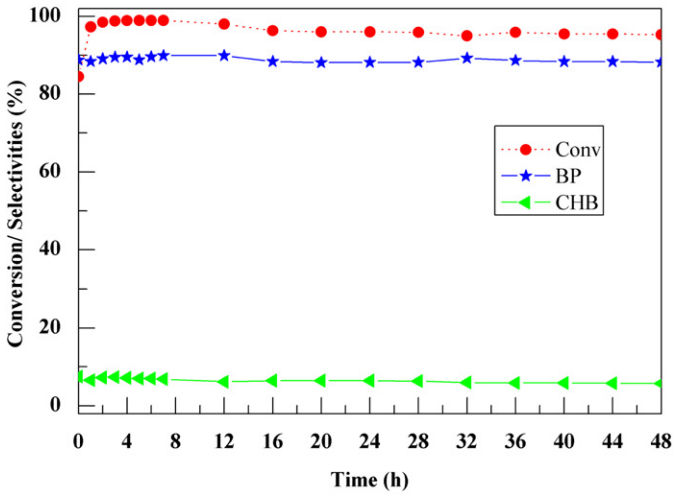

Fig. 8. Evolution of conversion and selectivity of different products as a function of time on stream for Ni_2P-10 catalyst at 400 °C.

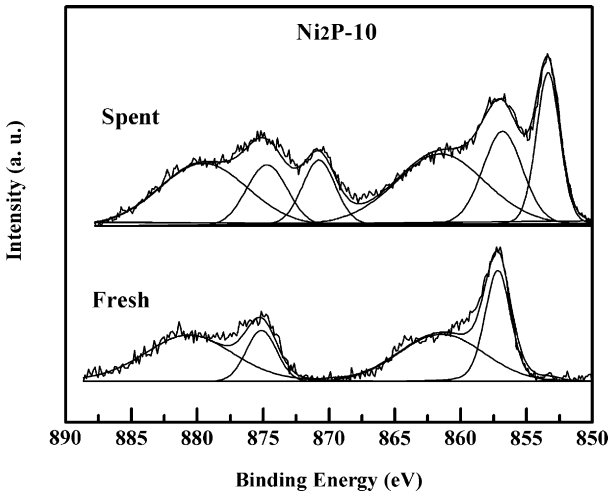

Fig. 9. Ni 2*p* core level spectra for Ni_2P-10 catalysts: (A) reduced catalysts and (B) spent catalysts after 48 h on time on stream.

higher binding energy values (853.7 eV), what suggests a strongest interaction of little particles with support that generates an electronic deficiency on Ni_2P particles favoring so its interaction with sulfur atoms possibly forming a superficial phosphosulfide phase. However, the adsorption of sulfur on Ni_2P-10 and Ni_2P-15 samples with higher particles sizes, should not be precluded [55]. The adsorption of sulfur on these samples should be weak and easier to be hydrogenated to remove sulfur as H_2S, meanwhile the phosphorous excess interacting with the support, could have the function of keeping the supported Ni_2P fully phosphided, thus facilitating high TOFs [31]. Besides, although XPS analysis has been carried out without exposure to air, a partial passivation cannot be avoided and therefore hindering sulfur detection on these samples. Oyama et al. [51] pointed the absence of sulfur on Ni_2P/SiO_2 spent catalysts to the lack of sensitivity by XPS at the levels expected for surface sulfur species in these supported samples. In the same way, Oyama et al. [17] reported that the smaller the Ni_2P particles the greater the degree of sulfidation. Results exposed in this work agree with this statement, as Ni_2P-5 catalyst, with the lowest particle size, possesses a higher degree of sulfidation. On bigger particles, the extent of sulfidation is lesser and sulfur atoms forming a phosphosulfide phase are easier to be hydrogenated to be removed as H_2S.

From results compiled in Table 3 and exposed before, it can be seen that Ni_2P-15 catalyst clearly has an excess of metallic loading that is unnecessary. Ni_2P-10 catalyst, with an intermediate morphology and metallic loading, was chosen to further investigate the influence of reaction time. With this purpose in mind, the time course of HDS activity for Ni_2P-10 catalyst was performed for 48 h. Fig. 8 shows the conversion and yield values versus reaction time. The reaction temperature chosen was 400 °C. Fig. 8 gathers together the corresponding results. It can be seen that Ni_2P-10 catalyst improves its catalytic capacity with time on stream, which suggests that the amount of Ni_2P is increased and/or the formation of an intermediate phase which is more active than Ni_2P occurs. As before, BP is the main product formed. The increasing activity during the reaction time in the initial stage as well as the catalyst stability, have previously been observed [20,21,56]. Sun et al. [43] have reported that the surface of phosphide catalysts evolve into a more active form with time on stream, while the structure of phosphides can be preserved in HDS reactions. Korányi [22] observed an increase in tiophene HDS activity of prereduced phosphates ($Ni_3(PO_4)_2$) as a consequence of its transformation to more active Ni_2P phase under the given reaction conditions.

The surface modification of Ni_2P phase during the catalytic test and the explanation of its excellent behavior with time on stream have been considered in the literature as consequence of the presence of a superficial phosphosulfide as active phase [19,43,57,58] with a stoichiometry represented by NiP_xS_y. Theoretical studies carried out by Nelson et al. [58] indicated that the stoichiometry of the phosphosulfide on the surface of Ni_2P is Ni_3PS. Another phosphosulfide formed on the surface of Ni_2P particles found by some authors is $NiPS_3$, which has been reported to be a very active phase [59]. However, Korányi [22] studied bulk $NiPS_3$ in thiophene HDS and emphasized its low HDS activity due to a low specific surface area, although thiophene HDS mixture transform it into active Ni_2P compound. In a recent study of Ni_2P/SBA catalysts, Korányi et al. [52] reported the presence of a superficial phosphosulfide with a composition $Ni_{2.4}P_{1.0}S_{0.24}$ as responsible of the activity.

In an attempt to elucidate the behavior of Ni_2P-10 catalyst, a characterization of the spent catalyst was carried out with XRD, XPS and CNHS experiments. XRD results for this sample (not shown) confirm the formation of an ever more crystalline Ni_2P phase, with a particle size of 137 nm. TOF value for this catalyst is 0.016 s^{-1}, as consequence of lower metal site density (13.1 μmol g^{-1}), and corroborates the structure insensitivity on this catalyst. CNHS reveals very low sulfur content after the catalytic test (0.014 wt%). XPS measurements of Ni 2*p* signal for this spent catalyst is shown in Fig. 9, where a comparison between the signal of fresh and spent catalyst is made. Focusing our attention on Ni_2P band (~853.0 eV), the most striking result is the sharp increase in intensity of this band. This corroborates the formation of more active Ni_2P phase, which is also more crystalline, as previously stated and reported by other authors [17]. The formation of more Ni_2P under reaction conditions reveals that only a partial reduction occurs in the H_2 treatment prior to the catalytic test, and is responsible for the increasing activity of Ni_2P-10 catalyst. The Ni/P ratio increases for this spent catalyst. Further, no sulfur was detected from XPS analysis. On supported nickel phosphide samples, the formation of a superficial phosphosulfide as the active phase is fully documented in the literature, as stated before. A little passivation along with the low capacity of this sample to strongly retain sulfur, due to its high particle size, could be responsible of such absence. An indicative of the presence of sulfur retained on Ni_2P surface could come from Ni $2p_{3/2}$ shake-up satellite, which should have decreased if more Ni_2P is formed, as this compound contributes much less to this satellite, nonetheless it increases with regards reduced catalysts (Figs. 7 and 9). Some authors have pointed that the presence of this band could be due to

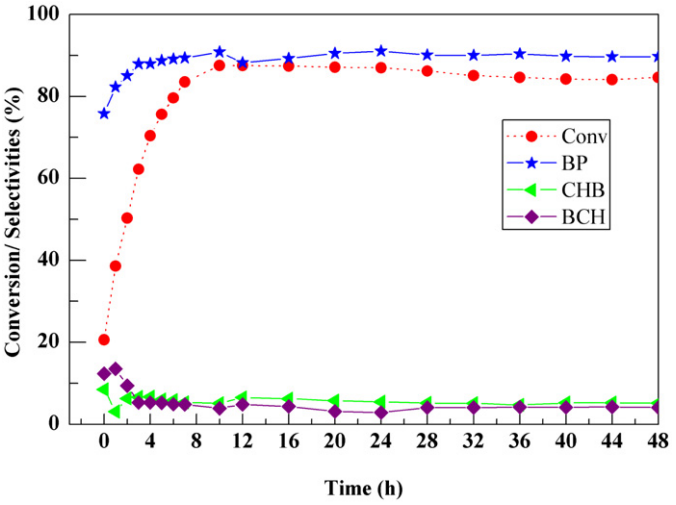

Fig. 10. Evolution of conversion and selectivity of different products as a function of time on stream for $Ni(HPO_3H)_2$/MCM-41 sample at 400 °C.

the presence of oxysulfided nickel species [47] and is indicative of the presence of retained sulfur species on nickel atoms.

Considering the results previously presented for Ni_2P-10 catalyst, which shows an increasing activity during reaction due to the formation of more Ni_2P phase, a new trial was carried out to study the catalytic activity of the precursor catalyst with a 10 wt% of nickel, $Ni(HPO_3H)_2$ supported on MCM-41, without a prior reduction and the corresponding results are plotted in Fig. 10. It is surprising how the activity appears with time on stream, which increases monotonically over the course of 48 h, reaching 87.5% conversion after 10 h of reaction. The conversion tends to a constant value of 84.0%. Similar behavior was observed by Sawhill et al. [21] but using phosphate species as precursors. An increase in activity with time on stream was observed as a consequence of the formation of phosphide/phosphosulfide phase under the reducing conditions present in HDS reactor. However, the increase in activity observed for our precursor is much more significant, with a conversion pattern, after 48 h on stream, very close to the same sample pre-treated under a H_2 flow. The better reducibility of phosphite precursor is responsible for such behavior.

XRD analysis of this spent catalyst shows the diffraction lines arising from the presence of Ni_2P, revealing the formation of a Ni_2P active phase during the reaction. The particle size obtained is 94 nm, lower than the same sample prior reduced. This particle size provided a TOF of 6.2 10^{-3} s^{-1}, which confirms the intrinsic catalytic activity of this sample. The presence of Ni_2P is also detected from XPS results for this sample (Fig. 11A), where the Ni $2p_{3/2}$ peak at 852.8 eV is clearly identified. The formation of the desired nickel phosphide takes place during the catalytic test. Notwithstanding, the Ni $2p$ signal is very noisy, as is the case for Ni_2P-5 spent catalyst. In both cases the Ni/P atomic ratio is very low. This fact, along with the appearance of the S $2p$ bands located at 162.5 and 169.6 eV (Fig. 11B) with a superficial atomic concentration of 3.6 wt%, indicate again that superficial phosphosulfide is formed over this sample. This phase (NiP_xS_y) is formed in a greater extent as a consequence of the experimental conditions employed which are different to those used to reduce the precursor in absence of sulfur compounds.

4. Conclusions

Nickel phosphide, Ni_2P, catalysts were prepared by hydrogen reduction of nickel(II) dihydrogenphosphite, an X-ray amorphous precursor, and by using a silica mesoporous material such as MCM-41 as material support. The optimized experimental conditions

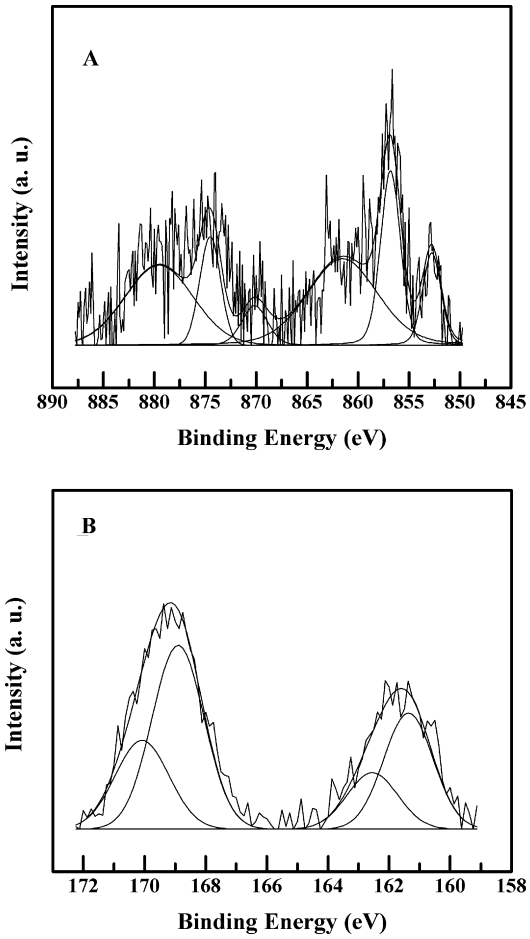

Fig. 11. Ni $2p$ (A) and S $2p$ (B) core level spectra for $Ni(HPO_3H)_2$/MCM precursor catalyst after 48 h on stream.

were: 3 °C min^{-1} of heating rate, 100 ml min^{-1} of H_2 flow and 375 °C of reduction temperature. The method supposes an energy saving as there is no need of calcination and a lower reduction temperature is required. Notwithstanding, a high loading of nickel and phosphorous in the catalyst favors the formation of mixed phases and destroys the mesoporous structure. Nickel phosphide catalysts prepared by this method proved to be highly active in DBT HDS. The stability of these catalysts is high, with no deactivation observed during 48 h time on stream whilst displaying an improved conversion of close to 100% with high selectivity of biphenyl (BP). The analysis of spent catalysts shows that the particle size is a clue to retain more or less sulfur during the test. In this sense Ni_2P-5 catalyst hardly modifies its particle size and retains more sulfur in the form of phosphosulfide than Ni_2P-10 and Ni_2P-15 spent samples, which due to an increase of the Ni_2P crystallite size retain less superficial sulfur during the test. This fact along with a partial passivation hinders the sulfur detection. The ensemble size does not modifies HDS activity (Structure insensitive) but favors nickel sites regeneration by hydrogenation. Moreover $Ni(HPO_3H)_2$/MCM-41 precursor catalyst, without a prior reduction, possesses an increasing catalytic activity with time on stream as a consequence of the formation of Ni_2P phase under reaction condition which is covered by a phosphosulfide NiP_xS_y phase, as detected by XPS. However this sample reaches a conversion value after 48 h on stream slightly lower than the same sample with a reduction treatment prior to the catalytic test possibly due to the presence of strongly adsorbed sulfur atoms that can be blocking Ni sites.

Acknowledgments

We gratefully acknowledge the support from Ministerio de Educación y Ciencia through the Project MAT2006-02465 and from Junta de Andalucía through the Excellence Project P06-FQM-01661. J.A.C.B. thanks Ministerio de Educación y Ciencia (Spain) for a fellowship (BES-2007-15735). A.I.M. also thanks Junta de Andalucía for a postdoctoral contract. The authors are very pleased to Professor S. Ted Oyama for his helpful suggestions.

References

[1] http://www.eia.doe.gov/oiaf/aeo/assumption/petroleum.html.
[2] E. Rodríguez-Castellón, A. Jiménez-López, D. Eliche-Quesada, Fuel 87 (2008) 1175.
[3] B. Pawelec, J.L.G. Fierro, A. Montesinos, T.A. Zepeda, Appl. Catal. B 80 (2008) 1.
[4] R. Nava, J. Morales, G. Alonso, C. Ornelas, B. Pawelec, J.L.G. Fierro, Appl. Catal A 321 (2007) 58.
[5] S.K. Maity, G.A. Flores, J. Ancheyta, M.S. Rana, Catal. Today 130 (2008) 374.
[6] J.M. Lewis, R.A. Kydd, R.M. Boorman, P.H. van Rhyn, Appl. Catal A 84 (1992) 103.
[7] R. Prins, Adv. Catal. 46 (2002) 399.
[8] P.J. Magnus, A.D. van Langeveld, V.H.J. de Beer, J.A. Moulijn, Appl. Catal A 68 (1991) 161.
[9] R. Prins, V.H.J. de Beer, G.A. Somorjai, Catal. Rev. Sci. Eng. 31 (1989) 1.
[10] S. Gong, H. Chen, W. Li, B. Li, Appl. Catal. A 279 (2005) 257.
[11] M. Nagai, Appl. Catal. A 322 (2007) 178.
[12] M. Lewandowski, A. Szymańska-Kolasa, P. Da Costa, C. Sayag, Catal. Today 119 (2007) 31.
[13] S.T. Oyama, C.C. Yu, S. Ramanathan, J. Catal. 535 (1999) 184.
[14] V. Zuzaniuk, R. Prins, J. Catal. 219 (2003) 85.
[15] S.T. Oyama, P. Clark, X. Wang, T. Shido, Y. Iwasawa, S. Hayashi, J.M. Ramallo-Lopez, F.G. Requejo, J. Phys. Chem. B 106 (2002) 1913.
[16] C. Stinner, Z. Tang, M. Haouas, T. Weber, R. Prins, J. Catal. 208 (2002) 456.
[17] S.T. Oyama, X. Wang, Y.K. Lee, K. Bando, F.G. Requejo, J. Catal. 210 (2002) 207.
[18] S.T. Oyama, X. Wang, F.G. Requejo, T. Sato, Y. Yoshimura, J. Catal. 209 (2002) 1.
[19] S.T. Oyama, J. Catal. 216 (2003) 343.
[20] J.A. Rodriguez, J.Y. Kim, J.C. Hanson, S.J. Sawhill, M.E. Bussell, J. Phys. Chem. B 107 (2003) 6276.
[21] S.J. Sawhill, D.C. Phillips, M.E. Bussell, J. Catal. 215 (2003) 208.
[22] T. Korányi, Appl. Catal. A 239 (2003) 253.
[23] M.J. Ledoux, O. Michaux, G. Agostini, J. Catal. 102 (1986) 275.
[24] P.J. Mangnus, A. Riezebos, A.D. van Langeveld, J.A. Moulijn, J. Catal. 151 (1995) 178.
[25] J. Frimmel, M. Zdrazil, J. Catal. 167 (1997) 286.
[26] J. Quartararo, S. Mignard, S. Kasztelan, J. Catal. 192 (2000) 307.
[27] F. Nozaki, M. Tokumi, J. Catal. 79 (1983) 207.
[28] R.L. Ripley, J. Less-Common Met. 4 (1962) 496.
[29] A.R. West, Solid State Chemistry and its Applications, Wiley, Chichester, 1992.
[30] M. Chene, Ann. Chim. 15 (1941) 187.
[31] S.J. Sawhill, K.A. Layman, D.R. Van Wyk, M.H. Engelhardb, C. Wang, M.E. Bussel, J. Catal. 231 (2005) 300.
[32] Y. Shu, S.T. Oyama, Carbon 43 (2005) 1517.
[33] H. Loboué, C. Guillot-Deudon, A.F. Popa, A. Lafond, B. Rebours, C. Pichon, T. Cseri, G. Berhault, C. Geantet, Catal. Today 130 (2008) 63.
[34] S. Yang, C. Liang, R. Prins, J. Catal. 237 (2006) 118.
[35] A.E. Henkes, Y. Vasquez, R.E. Schaak, J. Am. Chem. Soc. 129 (2007) 1896.
[36] R.K. Chiang, R.T. Chiang, Inorg. Chem. 46 (2007) 369.
[37] U. Ciesla, F. Schüth, Microporous Mesoporous Mater. 27 (1999) 131.
[38] C. Stinner, R. Prins, Th. Weber, J. Catal. 202 (2001) 187.
[39] P. Burattin, M. Che, C. Louis, J. Phys. Chem. B 104 (2000) 10482.
[40] S.T. Oyama, Y.-K. Lee, J. Catal. 258 (2008) 393.
[41] J.B. Parise, Acta Crystallogr. 36 (1980) 1179.
[42] I.I. Abu, K.J. Smith, Appl. Catal. A 328 (2007) 58.
[43] F. Sun, W. Wu, Z. Wu, J. Guo, Z. Wei, Y. Yang, Z. Jiang, F. Tian, C. Li, J. Catal. 228 (2004) 298.
[44] D. Kanama, S.T. Oyama, S. Otani, D.F. Cox, Surf. Sci. Spectra 8 (2001) 220.
[45] D. Eliche-Quesada, J. Mérida-Robles, P. Maireles-Torres, E. Rodríguez-Castellón, A. Jiménez-López, Langmuir 19 (2003) 4985.
[46] J.N. Kuhn, N. Lakshminarayanan, U.S. Ozkan, J. Mol. Catal. A 282 (2008) 9.
[47] N. Escalona, J. Ojeda, P. Baeza, R. García, J.M. Palacios, J.L.G. Fierro, A. López Agudo, F.J. Gil–Llambías, Appl. Catal. A 287 (2005) 47.
[48] A. Bertrand, J. Vac. Sci. Technol. 18 (1981) 28.
[49] I.I. Abu, K.J. Smith, J. Catal. 241 (2006) 356.
[50] K.A. Layman, M.E. Bussell, J. Phys. Chem. 102 (1998) 6986.
[51] X. Wang, P. Clark, S.T. Oyama, J. Catal. 208 (2002) 321.
[52] T.I. Korányi, Z. Vít, D.G. Poduval, R. Ryoo, H.S. Kim, E.J.M. Hensen, J. Catal. 253 (2008) 119.
[53] J.F. Moulder, W.F. Stickle, P.E. Sool, K.D. Bomber, Handbook of X-Ray Photoelectron Spectroscopy, Perkin–Elmer, Eden Prairie, MN, 1992.
[54] X. Duan, Y. Teng, A. Wang, V.M. Kogan, X. Li, Y. Wang, J. Catal. 261 (2009) 232.
[55] P. Liu, J.A. Rodríguez, T. Asakura, J. Gomes, K. Nakamura, J. Phys. Chem. B 109 (2005) 4575.
[56] D.C. Phillips, S.J. Sawhill, R. Self, M.E. Bussell, J. Catal. 207 (2002) 266.
[57] T. Kawai, K.K. Bando, Y.-K. Lee, S.T. Oyama, W.-J. Chun, K. Asakura, J. Catal. 241 (2006) 20.
[58] A.E. Nelson, M. Sun, A.S.M. Junaid, J. Catal. 241 (2006) 180.
[59] A. Andreev, C. Vladov, L. Prahov, P. Atanasova, Appl. Catal. A 108 (1994) 97.